

* Work supported in part by the National Science Foundation and U.S. Office of Naval Research Contract No. N00014-69-0200-4006.

¹ M. B. Walker, Phys. Rev. B **1**, 3690 (1970).

² H. J. Spencer and R. Orbach, Phys. Rev. **179**, 683 (1969); R. Orbach and H. J. Spencer, *ibid.* **179**, 690 (1969).

³ J. Dupraz, B. Giovannini, R. Orbach, J. D. Riley, and J. Zitkova, in *Proceedings of the International Conference on Electron and Nuclear Magnetic Resonance, Monash University, 1969* (Plenum, New York, 1970), p. 197. Because of an unfortunate error, acknowledgment was not made in this reference to the work of Dr. N. Rivier (private communication). He was responsible for the analytic form for $\chi^-(\omega)$ [Eq. (2.9)] used to discuss the magnetic-resonance bottleneck and should have been included as a coauthor.

⁴ A. A. Abrikosov, Physics **2**, 5 (1965); **2**, 61 (1965).

⁵ H. J. Spencer, Phys. Rev. **171**, 515 (1968).

⁶ An analogous investigation, appropriate to optical-phonon-electron interactions, has been carried out by S. Engelsberg and J. R. Schrieffer, Phys. Rev. **131**, 993 (1963).

⁷ H. J. Spencer and S. Doniach, Phys. Rev. Letters **18**, 994 (1967); Ref. 5 of this paper; D. C. Langreth, D. L. Cowan, and J. W. Wilkins, Solid State Commun. **6**, 131 (1968).

⁸ This is because the high-temperature limits of both the real and imaginary parts of the localized and conduction-electron self-energies are frequency independent. Hence, convolution of the Green's functions to obtain the transverse susceptibility amounts to nothing more than the addition of the imaginary part of the single-particle self-energies when computing the line-width, and the subtraction of the real parts when computing the line shift.

⁹ T. Holstein, Ann. Phys. (N.Y.) **29**, 410 (1964).

¹⁰ P. Fulde and A. Luther, Phys. Rev. **170**, 570 (1968); **175**, 337 (1968).

Faraday Rotation near the Ferromagnetic Critical Temperature of CrBr₃†

JOHN T. HO

Department of Physics and Laboratory for Research in the Structure of Matter, University of Pennsylvania, Philadelphia, Pennsylvania 19104

AND

J. D. LITSTER

Department of Physics and Center for Materials Science and Engineering, Massachusetts Institute of Technology, Cambridge, Massachusetts 02139

(Received 17 July 1970)

We have used the Faraday effect to measure the magnetization of the insulating ferromagnet CrBr₃ as a function of magnetic field (up to 9.5 kG) along 29 isotherms in the temperature range $T_c - 2.8^\circ\text{K} < T < T_c + 6.7^\circ\text{K}$, where $T_c = 32.884^\circ\text{K}$. The numerical results are presented in tabular form. We have also analyzed these data and found that the spontaneous magnetization goes to zero as $(T_c - T)^\beta$ with $\beta = 0.368 \pm 0.005$. Along the critical isotherm $M \sim H^{1/\delta}$ with $\delta = 4.28 \pm 0.1$ and the susceptibility for $M = 0$ and $T > T_c$ diverges as $(T - T_c)^{-\gamma}$ with $\gamma = 1.215 \pm 0.02$. All of the data are consistent with the hypothesis of the static scaling laws. Two simple parametric equations of state were tried, and the better of the two was found to represent the data quite well and be a useful form for calculations of thermodynamic properties in the critical region.

I. INTRODUCTION

The striking similarities in the anomalous behavior of thermodynamic properties near phase transitions in apparently very different materials has led to intense experimental and theoretical interest in the study of magnetic materials, fluids, and other substances in the region around the critical point.¹⁻³

The first general model of the critical point was provided by Landau's theory of second-order phase transitions,⁴ which is equivalent to the Weiss molecular-field model for magnetic systems or to the van der Waals equation for fluids. The Landau model assumes the free energy to be analytic everywhere in the critical region, and predicts thermodynamic anomalies at the critical point which are qualitatively valid but which have been experimentally shown to be quantitatively incorrect. The physical reason for this is clear: The Landau model predicts a diverging susceptibility at the critical point, but fails to include the diverging fluctuations of the order parameter (magnetization) which accompany the rise in susceptibility.

A significant unifying advancement was the concept of static scaling laws⁵⁻⁷ based upon the physical idea that the fluctuations in order parameter could be treated by means of a spatial correlation function with the critical behavior expressed as the divergence of a single correlation length at the critical point. This leads to the mathematical assumption that the free energy is everywhere analytic except at the critical point itself (and possibly along the coexistence curve). Expressed in magnetic language, the static scaling laws may be summarized in the statement that the scaled magnetic field $H | T - T_c |^{-\beta\delta}$ is a function only of the scaled magnetization $M | T - T_c |^{-\beta}$ (where β , δ are the usual critical exponents along the coexistence curve and critical isotherm, respectively). That is,

$$H | T - T_c |^{\beta\delta} = \Phi(M | T - T_c |^\beta). \quad (1)$$

These ideas were first experimentally tested and verified within the accuracy of available data for the metallic ferromagnets nickel^{8,9} and CrO₂ (only for $T > T_c$).¹⁰ The analysis of data collected by Green,

Vicentini-Missoni, and Sengers¹¹ is consistent with the scaling law hypothesis for pure fluids.

In this paper we present the results of our measurements of the equilibrium properties of the insulating ferromagnet CrBr_3 . A preliminary analysis of our data showed the scaling laws to be valid within experimental errors, and this provided the first experimental confirmation of the scaling hypothesis for an insulating ferromagnet.¹² Our measurements were sufficiently precise to enable the determination of the form of the scaling function Φ in Eq. (1), and we gave several mathematical representations for the equation of state in a previous letter.¹³ In the present paper we discuss the details of our experiment, give the numerical results of our measurements, and include a discussion of the analysis of the experimental results that was omitted from our earlier reports because of limitations of space. We also present the results of data analysis to test parametric equations of state^{14,15} that we have carried out since the publication of our preliminary results.

II. EXPERIMENTAL

It is desirable to study an insulating ferromagnet, such as CrBr_3 ,¹⁶ because the Heisenberg model for ferromagnetism assumes the magnetic moments to be localized on a lattice. Comparison with theory is therefore more meaningful than for metallic magnets with their mobile magnetic moments.

Zero-field nuclear magnetic resonance^{17,18} provides the most accurate method to measure magnetization in many magnetic systems. This method has been applied to CrBr_3 in the critical region¹⁹ to measure the temperature dependence of the spontaneous magnetization (i.e., the shape of the coexistence curve). Unfortunately this technique does not provide measurements of the magnetization as a function of magnetic field and cannot be used for temperatures very close to the critical temperature. The more conventional force²⁰ or induction²¹ methods include undesirable moving parts and require rather large uniform samples. Complications arise when the sample is magnetically anisotropic, as is CrBr_3 . These methods would require a large single crystal of CrBr_3 , which is not available.

Fortunately, CrBr_3 is somewhat transparent to visible light and exhibits a large Faraday rotation proportional to the magnetization.²² CrBr_3 crystals grow in the form of small thin flakes perpendicular to the hexagonal c axis, which is also the easy magnetization direction. We were therefore able to use the Faraday effect to study readily available single crystals with the field applied along the axis of easy magnetization. The use of a remote optical probe greatly simplified the temperature control of the sample.

Our measurements were made using light of wavelength 5461 Å selected from a mercury arc spectrum by means of a narrow-band interference filter. At this wavelength, CrBr_3 exhibits a large specific rotation and yet is reasonably transparent. We constructed a sensi-

tive polarimeter by modulating the plane of polarization of the incident light and using phase-sensitive detection to determine when the polarizer and analyzer were crossed.

The incident light was polarized by means of sheet Polaroid (type HN32), and the plane of polarization was rotated by means of a KDP Pockels cell and quarter-wave plate. The light then passed through the sample, a Glan-Thompson analyzer, and into a photomultiplier tube (RCA type 7265). The KDP cell was modulated at 500 Hz and a minimum in the 500-Hz component of the photomultiplier current (detected by means of a lock-in amplifier) indicated when the analyzer was crossed with the polarization of the light emerging from the sample. The amplitude of the modulation of the plane of polarization that is necessary for optimum signal-to-noise ratio is discussed in Appendix A. It is determined by the ratio of the transmitted light intensity with the polarizer and analyzer in the crossed and parallel orientations. In practice, the optimum amount of modulation was determined by adjusting polarizer and analyzer for minimum transmission with no modulation present. The modulation was then increased until at least a twofold increase in dc photocurrent was observed. We originally attempted to measure the Faraday rotation of the CrBr_3 by measuring the dc bias on the KDP cell that would just cancel out the rotation caused by the sample. However, the KDP cell was not stable under dc conditions and so we mounted the analyzer on the divided circle obtained from a transit. With this equipment, the light transmitted by a 20- μ -thick crystal of CrBr_3 was enough to enable us to measure rotations less than 10^{-4} rad. The saturated rotation of this sample was about 1.2 rad at 0°K, so we were able to measure magnetization changes of 10^{-4} of the saturation magnetization at 0°K. This sensitivity is about a factor of 3 less than that obtainable with zero-field NMR measurements, and with suitable samples and light sources the Faraday rotation method should surpass the sensitivity of NMR.

The sample was mounted in a copper block that also contained a germanium resistance thermometer, a carbon thermistor, and a heater. The copper block was thermally loosely coupled by means of a variable-pressure exchange gas to the helium reservoir of an optical Dewar. An electronic servo system with a fast proportional and a slow integral response regulated the heater power to keep the carbon thermistor at constant temperature. Temperatures from 25 to 40°K were obtained with a few mW of heater power. We checked for temperature gradients by adjusting the exchange-gas pressure so the system would regulate at the same temperature with varying amounts of heater power. For a given magnetic field and germanium thermometer reading, the CrBr_3 always showed the same rotation, indicating no significant temperature gradients for the heater power levels used. The servo maintained the

TABLE I. T , σ , and H data of CrBr_3 .

T ($^{\circ}\text{K}$)	σ	H (G)	T ($^{\circ}\text{K}$)	σ	H (G)
30.076	0.4895	82.3	32.826	0.1614	32.8
30.076	0.4956	262.6	32.826	0.1820	60.1
30.076	0.5096	729.6	32.826	0.2009	93.5
30.076	0.5210	1176.9	32.826	0.2177	134.5
30.076	0.5401	2116.0	32.826	0.2330	180.9
30.076	0.5678	4039.2	32.836	0.1606	35.7
30.076	0.6031	7488.8	32.836	0.2176	134.9
30.683	0.4681	529.1	32.836	0.2817	412.6
30.683	0.4909	1249.1	32.836	0.3317	838.1
30.683	0.5085	1980.1	32.836	0.3857	1649.5
30.683	0.5413	3880.8	32.836	0.4223	2525.7
31.925	0.3329	33.2	32.836	0.4709	4359.3
31.925	0.3500	170.9	32.836	0.5259	7751.5
31.925	0.3652	329.8	32.840	0.1370	18.5
31.925	0.3780	489.8	32.840	0.1600	37.3
32.106	0.3185	85.3	32.840	0.1808	64.3
32.106	0.3366	221.7	32.840	0.1992	99.5
32.106	0.3521	370.7	32.840	0.2159	140.7
32.106	0.3661	534.9	32.840	0.2314	186.1
32.286	0.2788	22.8	32.844	0.1376	17.8
32.286	0.3034	138.7	32.844	0.1814	63.3
32.286	0.3223	268.1	32.844	0.2171	138.1
32.286	0.3394	421.4	32.844	0.2818	420.8
32.286	0.3532	570.3	32.844	0.3430	984.7
32.478	0.2628	80.5	32.844	0.3920	1802.8
32.478	0.2872	190.8	32.844	0.4261	2672.9
32.478	0.3078	322.6	32.844	0.4523	3584.9
32.478	0.3256	467.3	32.844	0.4739	4546.0
32.478	0.3407	619.7	32.844	0.4910	5479.5
32.589	0.2202	25.2	32.844	0.5195	7398.4
32.589	0.2370	66.0	32.852	0.1110	10.1
32.589	0.2521	112.6	32.852	0.1359	22.3
32.637	0.2164	38.8	32.852	0.1588	41.9
32.637	0.2335	78.6	32.852	0.1795	69.1
32.637	0.2488	125.1	32.852	0.1980	103.6
32.655	0.1953	13.8	32.852	0.2146	145.3
32.655	0.2149	44.8	32.855	0.1594	39.2
32.655	0.2318	85.2	32.855	0.2162	139.2
32.655	0.2471	131.6	32.855	0.2798	418.6
32.676	0.1938	19.0	32.855	0.3309	841.3
32.676	0.2135	49.8	32.855	0.3817	1668.4
32.676	0.2306	89.7	32.855	0.4218	2533.3
32.676	0.2441	141.9	32.855	0.4712	4380.3
32.709	0.1913	28.3	32.855	0.5260	7774.6
32.709	0.2106	60.2	32.858	0.1363	21.3
32.709	0.2275	100.7	32.858	0.1591	41.0
32.709	0.2429	146.5	32.858	0.1798	68.1
32.768	0.1653	19.6	32.858	0.1982	103.2
32.768	0.1865	45.0	32.858	0.2149	144.4
32.768	0.2054	78.5	32.858	0.2303	190.1
32.768	0.2222	119.6	32.872	0.1110	11.7
32.768	0.2374	165.9	32.872	0.1354	25.7
32.822	0.1383	14.2	32.872	0.1578	46.8
32.822	0.1616	32.0	32.872	0.1783	74.6
32.822	0.1825	58.6	32.872	0.1968	109.5
32.822	0.2013	92.5	32.872	0.2134	151.0
32.822	0.2179	133.8	32.872	0.2288	197.1
32.822	0.2333	179.9	32.926	0.0825	11.1
32.826	0.1381	14.8	32.926	0.1080	22.1

TABLE I (Continued)

T (°K)	σ	H (G)	T (°K)	σ	H (G)
32.926	0.1319	37.9	33.142	0.1754	183.6
32.926	0.1541	59.6	33.142	0.1916	226.4
32.926	0.1743	88.7	33.739	0.0187	35.2
32.926	0.1926	124.1	33.739	0.0371	70.6
32.926	0.2092	165.6	33.739	0.0728	145.0
32.926	0.2247	211.1	33.739	0.0897	185.2
32.981	0.0539	11.1	33.739	0.1063	226.9
32.981	0.0799	19.6	33.739	0.1221	271.3
32.981	0.1047	32.3	33.739	0.1372	318.2
32.981	0.1280	50.3	33.739	0.1517	367.2
32.981	0.1497	73.8	35.029	0.0221	122.4
32.981	0.1696	103.8	35.029	0.0331	183.7
32.981	0.1878	139.8	35.029	0.0440	245.2
32.981	0.2044	181.4	35.029	0.0548	307.2
33.034	0.0528	15.7	35.029	0.0654	369.8
33.034	0.0782	26.3	35.029	0.0760	432.5
33.034	0.1024	41.2	35.029	0.0864	496.0
33.034	0.1252	60.8	35.029	0.0965	560.4
33.034	0.1466	85.5	36.730	0.0207	230.0
33.034	0.1661	116.8	36.730	0.0343	382.0
33.034	0.1842	153.2	36.730	0.0477	534.7
33.034	0.2004	195.9	36.730	0.0611	687.6
33.034	0.2158	241.7	36.730	0.0871	998.8
33.142	0.0252	12.4	36.730	0.1240	1475.4
33.142	0.0498	25.8	39.517	0.0119	260.0
33.142	0.0736	42.0	39.517	0.0197	432.4
33.142	0.0966	61.1	39.517	0.0275	604.8
33.142	0.1183	84.5	39.517	0.0353	777.5
33.142	0.1387	112.6	39.517	0.0509	1127.0
33.142	0.1577	145.8	39.517	0.0740	1662.5

temperature constant to better than the sensitivity of our thermometer. Our germanium thermometer was calibrated against a platinum resistance thermometer used in previous NMR studies of CrBr_3 in the critical region.¹⁹ The absolute calibration is probably ± 20 mdeg and the relative temperatures are accurate to ± 2 mdeg.

Magnetic fields up to 9.5 kG were obtained in a 12-in. electromagnet and measured to 0.1% accuracy with a rotating coil gaussmeter and a Hall probe.

III. RESULTS AND ANALYSIS

The analysis of our measurements is based upon the assumption that the Faraday rotation Θ is directly proportional to the magnetization M of our sample. Therefore we write

$$\Theta = VM, \quad (2)$$

where V is a Verdet constant appropriate to the sample. In Appendix B we show that the linear relationship of Θ and M is expected theoretically. In addition to the theoretical justification, we were able to confirm this result experimentally.

The internal magnetic field of a ferromagnetic material is the difference between the external field and

the demagnetizing field. We used the demagnetizing field not only to verify Eq. (2), but also to obtain the numerical value of the Verdet constant. The internal field H_i for an infinitely thin disk is related to the applied field H_a by

$$H_i = H_a - 4\pi M. \quad (3)$$

For $T < T_c$ and M less than the saturation magnetization (this is analogous to the two-phase region for a fluid, the two phases being oppositely magnetized domains), we found no detectable hysteresis in the rotation and hence no magnetic hysteresis. The internal field was therefore zero and so the magnetization was given by $H_a/4\pi$. In this "two-phase region" the magnetization as a function of H_a was known and we were able to verify Eq. (2). For the sample on which measurements are reported here, we found for 5461-Å light the value of V was 4.935×10^{-3} rad $\text{erg}^{-1} \text{cm}^3 \text{G}$. There was no observable dependence of V upon temperature. Furthermore, outside of the coexistence curve (for $T > T_c$ or else M greater than saturation) the magnetization is given by

$$M = \chi H_i = \chi H_a / (1 + 4\pi\chi), \quad (4)$$

where χ is the susceptibility. In the immediate vicinity

of the critical point, $4\pi\chi \gg 1$, and so one obtains to a good approximation $M = H_a/4\pi$. From the initial slope of our M -versus- H_a curves, we were able to determine that V was independent of temperature up to about 100 mdeg above T_c . In particular, we observed no change in V on passing through the critical point. Therefore, the theoretical prediction that V is indeed a constant was verified to within the sensitivity of our measurements and the value $V = 4.935 \times 10^{-3}$ rad erg $^{-1}$ cm 3 G was used to analyze our data. Our crystal of CrBr $_3$ was not a perfect infinite disk; however, the calculated demagnetizing factor (for a sample 20 μ thick and 3.5 mm in diameter) is within 0.5% of the value 4π which we used. Were this correction applied, it would simply shift all our magnetization values by 0.5% and in no way alter our conclusions.

Since we believe others may wish to analyze our data, we present the results in numerical form in Table I. The reduced magnetization $\sigma = M/M(0^\circ\text{K})$ was obtained using the value $4\pi M(0^\circ\text{K}) = 3520$ G.²² We conservatively estimate the errors in internal field to be about ± 2 G, the reduced magnetization $\pm 10^{-4}$, and the temperatures ± 3 mdeg.

We first analyzed our data by a method similar to that employed by Kouvel and Fisher.²³ From a plot of σ^2 versus H/σ we extrapolated isotherms for $T > T_c$ to obtain the value of H/σ for $\sigma = 0$, which is the reciprocal of the susceptibility. If the susceptibility diverges as $(T - T_c)^{-\gamma}$, then a plot of $(1/\chi)^{1/\gamma}$ versus T should give a straight line passing through zero at T_c . We made such plots for various values of γ and from the plot which represented a straight line for the widest temperature range determined $\gamma = 1.215 \pm 0.02$ and $T_c = (32.844 \pm 0.01)^\circ\text{K}$. Extrapolating to zero field for $T < T_c$, we similarly found the shape of the coexistence curve to be given by $\beta = 0.368 \pm 0.005$, also with $T_c = (32.844 \pm 0.01)^\circ\text{K}$. Once T_c was known we were able to measure M versus H at 32.844°K and obtained $\delta = 4.28 \pm 0.1$. The uncertainty in the value of δ comes mostly from the uncertainty in T_c . For several isotherms near T_c , M appears to vary as $H^{1/\delta}$ within the experimental errors—however, the correct value of δ is obtained only if T_c is well known. For example, log-log plots of M versus H look quite linear for $T = T_c - 0.01^\circ\text{K}$ (giving $\delta = 4.4$) and $T_c + 0.02^\circ\text{K}$ ($\delta = 4.1$).

The value of β we find is in good agreement with $\beta = 0.365 \pm 0.015$ obtained by Senturia and Benedek¹⁹ by zero-field nuclear magnetic resonance. However our value of T_c is about 275 mdeg higher than that reported by Senturia and Benedek. Since we calibrated our thermometer against the one used by them, the discrepancy must be due to a difference in CrBr $_3$ samples. Similar variations of the critical temperature have been observed in nickel,^{8,9} yet the critical exponents obtained are in agreement with one another. Our sample was grown from the vapor phase using 99.9% chromium and analytical grade bromine. It has been suggested that impurities should cause a departure from the

power-law divergence of the susceptibility²⁴; we observe no departures to $(T - T_c)/T_c < 10^{-3}$. We also studied a second sample of CrBr $_3$ from a different preparation. Analysis of 12 isotherms for this sample yielded exponents and coefficients identical to those for our first sample, although the critical temperature was $(32.82 \pm 0.01)^\circ\text{K}$. The variation of T_c which has been observed for different samples should be considered in the design of proposed nuclear resonance thermometers using CrBr $_3$.¹⁹ We conclude that the power-law divergences we have measured represent, within experimental uncertainties, the true critical behavior of CrBr $_3$.

IV. EQUATION OF STATE

As we mentioned in the Introduction, the concept of static scaling laws predicts an equation of state of the form of Eq. (1). In a previous publication¹² we gave plots of scaled magnetic field and scaled magnetization that confirm this hypothesis for CrBr $_3$. Our measurements provided an experimental determination of the equation of state and were sufficiently precise to enable us to establish a mathematical representation for this equation. The results of several approaches were given in Ref. 13. We now wish to discuss details omitted from Ref. 13 and progress made since the appearance of our earlier paper.

Several approaches may be taken to obtain a mathematical representation for the equation of state. A successful representation using a relatively large number of parameters can be obtained by using power-series expansions about special paths such as the critical isochore and critical isotherm. We found three terms each in series (about the critical isochore and critical isotherm) adequately represented our data over the entire critical region. A second approach is to seek a single function to represent the function Φ of Eq. (1) over the entire critical region. This method has been tried with varying degrees of success by several authors.^{8,13,25} The most successful representation is the function used by Vicentini-Missoni, Green, and Sengers.²⁵

Although these approaches can provide a satisfactory representation of the experimental M , H , and T data, the resulting equation is not in a useful form for calculations in the critical region.

An equation of state which is mathematically elegant, clearly displays the relationships between various thermodynamic quantities in the critical region, and is particularly amenable to calculations of static thermodynamic properties can be obtained using the parametric approach suggested independently by Schofield¹⁴ and Josephsen.¹⁵ The parametric method is a general and powerful one that might profitably be used even in cases where the scaling laws do not apply. Here we confine ourselves to a discussion of two particular representations which are mathematically simple and

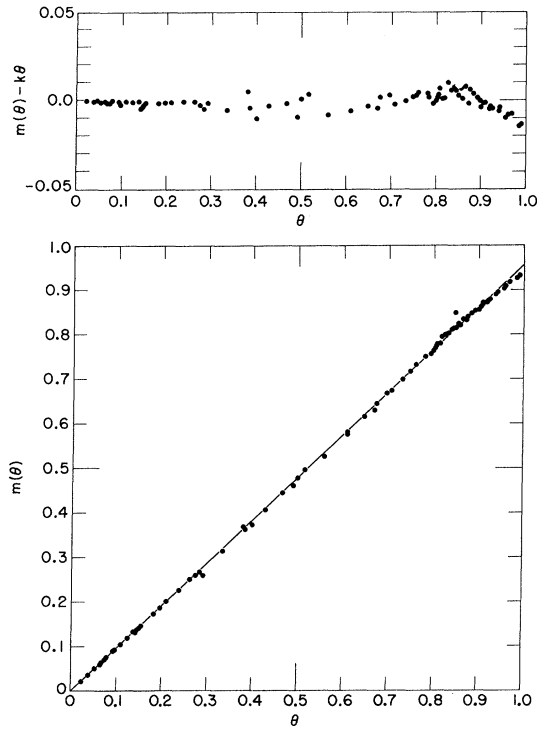


FIG. 1. Test of the equation of state (5). The lower portion of the figure shows the experimentally determined values of $m(\theta)$ in Eq. (C3b). The solid line is Eq. (5c) with $k=0.955$. Other parameters are given in the text. The upper portion of the figure shows the deviations of $m(\theta)$ from the solid line.

in which the parameters have a simple physical significance.

In the parametric representation of Schofield,¹⁴ a parameter r represents the "distance" from the critical point in the HT plane. It would be desirable to express this distance in some physically significant sense, say by having paths of constant r correspond to paths along which some thermodynamic quantity is constant. A quite satisfactory equation of state with this feature has already been presented.²⁶ The form of the equation of state is

$$H = a\theta(1-\theta^2)r^{\beta\delta}, \quad (5a)$$

$$T = (1-b^2\theta^2)r, \quad (5b)$$

$$M = k\theta r^\beta. \quad (5c)$$

The temperature origin is taken to be T_c and the scale factors a and k serve to convert magnetic field H and magnetization M into compatible units. When the parameter b^2 takes on the value

$$b^2 = (\delta-3)/(\delta-1)(1-2\beta), \quad (5d)$$

lines of constant r correspond to paths of constant specific heat C_M . The parameter r then measures the distance from the critical point in terms of mean squared fluctuations in energy density, and the correlation

function for energy density fluctuations depends only on r .

An alternative approach is to use the transformation

$$H = a\theta(1-\theta^2)r^{\beta\delta}, \quad (6a)$$

$$T = (1-b^2\theta^2)r, \quad (6b)$$

$$M = k\theta\{1 - [(3-2\beta\delta)/(3-2\beta)]\theta^2\}r^\beta \\ = k\theta(1-c\theta^2)r^\beta, \quad (6c)$$

$$b^2 = 3/(3-2\beta). \quad (6d)$$

With this equation of state, paths of constant r correspond to paths of constant susceptibility. Then r measures the distance from the critical point in terms of mean squared fluctuations in magnetization, and the correlation function for magnetization fluctuations depends only on the parameter r .

In either of these representations, the parameter θ locates a point in the HT plane along paths of constant specific heat [Eq. (5)] or susceptibility [Eq. (6)]. The critical isochore is $\theta=0$, the critical isotherm $\theta=\pm b^{-1}$, and the coexistence curve $\theta=\pm 1$. Both equations have only five adjustable parameters: T_c , β , δ , a , k . We used a computer program to vary simultaneously all five parameters for the best nonweighted least-squares fit to our CrBr_3 data. The resulting values for Eq. (5) were $\beta=0.366$, $\delta=4.34$, and $T_c=32.846$, in excellent agreement with the results of analysis along specific paths in the HT plane.¹² The magnetization was expressed in reduced units, as in Table I, and the temperature in reduced units by division by T_c . With the magnetic field in dimensionless units ($\hat{H} = g\mu_B SH/k_B T_c$) we obtained the values $a=0.875$, $k=0.955$. The results are illustrated in Fig. 1.

Using the alternative Eq. (6) we obtained the best fit with $\beta=0.372$, $\delta=4.36$, and $T_c=32.846$. With the same dimensionless units as for Eq. (5), the constants were $a=0.800$ and $k=0.765$. The results are shown in Fig. 2.

The deviations of the experimentally determined values of $m(\theta)$ from Eqs. (5c) and (6c) are also shown in Fig. 1 and 2, respectively. The relatively large deviations near the critical isotherm ($\theta=0.817$ and 0.795 , respectively, for the two figures) are caused by small temperature errors and are within experimental errors; Eq. (5) provides a satisfactory fit to the data everywhere except in the region near the coexistence curve. Here there is a small but systematic deviation as the coexistence curve ($\theta=1$) is approached; this is probably outside of the experimental uncertainties. Eq. (6), on the other hand, shows systematic deviations somewhat larger than experimental errors over the entire critical region.

We have also applied these equations to the pure fluids He^3 and He^4 , and either equation seems to represent the data satisfactorily.²⁷ For CrBr_3 , Eq. (5), while not perfect, is clearly preferable and provides a

satisfactory representation of our experimental data. For convenience we give in Appendix C the expressions for various thermodynamic quantities that are obtained using Eq. (5).

We should like to comment on the existence of "pseudospinodal" curves as discussed by Chu, Shoenes, and Fisher²⁸ for critical mixtures and Benedek²⁹ for SF₆. Experimentally it is often observed that a quantity (such as the susceptibility in a ferromagnet) which diverges as $(T-T_c)^{-\gamma}$ along the critical isochore will apparently diverge as $(T-T_c^*)^{-\gamma}$ along other isochores.¹² The locus of the temperatures T_c^* for various densities determines a pseudospinodal curve. In the van der Waals equation this curve coincides with the true spinodal curve of van der Waals, which is a curve of infinite compressibility (or susceptibility) and hence a boundary to a metastable region within the coexistence curve. Whether the true and pseudospinodal curves should coincide in general is not clear. However, we may see from the scaling hypothesis why the pseudospinodal behavior is experimentally observed. This is easily seen for the susceptibility in a ferromagnet. The equation of state may be represented as a power-series expansion about the critical isotherm ($T=0$) of the form¹³

$$H = b_0 M^\delta + b_1 T M^{\delta-1/\beta} + b_2 T^2 M^{\delta-2/\beta} + \dots \quad (7)$$

For CrBr₃ we found this series to represent the data quite adequately for all $T < 0$ and for a considerable portion of the critical region with $T > 0$. We also found the third term in the series to be relatively unimportant. If only the first two terms in Eq. (7) are considered, one readily obtains for the susceptibility along an isochore

$$\begin{aligned} (\chi)^{-1/\gamma} &= (\partial M / \partial H) T^{-1/\gamma} \\ &= [b_1(\beta\delta - 1) / b_0\beta^2\delta(\delta - 1)] T + (b_0\delta)^{1/\gamma} M^{1/\beta}. \end{aligned} \quad (8)$$

This apparently diverges at T_c^* , a temperature lower than T_c by an amount proportional to $M^{1/\beta}$ and therefore yields a pseudospinodal curve with the same exponent as the coexistence curve. Similar expressions for specific heat and susceptibility can be obtained from the parametric equation of state (5), and are given in Ref. 26. The range of temperatures for which this pseudospinodal behavior is observed depends upon the coefficients in the equation of state and therefore varies from substance to substance. We see from the discussion that a pseudospinodal curve with the same exponent as the coexistence curve is consistent with the scaling hypothesis. However, a parabolic pseudospinodal curve, as reported for SF₆, is not consistent with scaling.

V. SUMMARY AND CONCLUSIONS

We have shown that Faraday rotation can provide accurate measurements of magnetic properties in the critical region for suitable magnets, and have used this

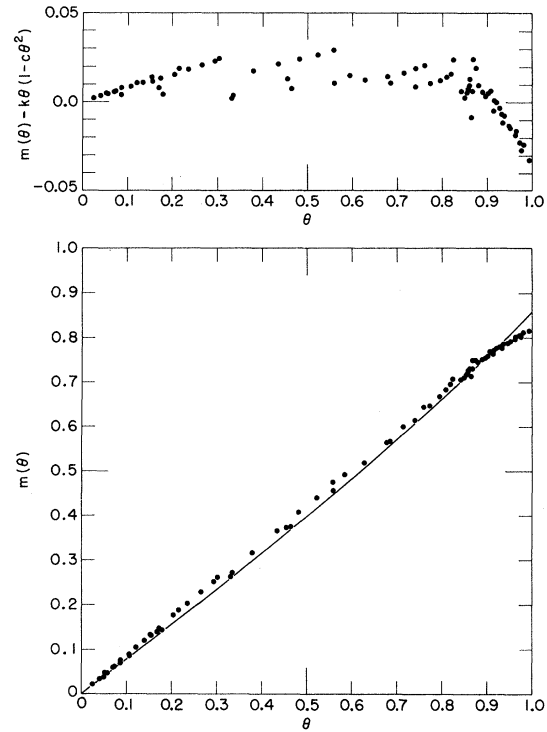


FIG. 2. Test of the parametric equation of state (6). The lower portion of the figure shows the experimental values of $m(\theta)$ in Eq. (C3b). The solid line is Eq. (6c) with $k=0.765$. Other parameters are given in the text. The upper portion of the figure shows the deviations of $m(\theta)$ from the solid line.

technique to study CrBr₃. Other materials under investigation include yttrium iron garnet, EuS, and EuO.

Measurements on CrBr₃ showed this insulating ferromagnet to be described within experimental error by the static scaling law hypothesis.

The parametric method appears to be the best approach to an equation of state. One can obtain a single equation that is valid over the entire critical region, possesses the mathematical properties required by the scaling hypothesis, and also adequately describes the experimental data using a minimum of adjustable constants.

We have tried two specific parametric representations for the equation of state that are mathematically simple and also have obvious physical interpretations. In one representation, Eq. (5), the distance from the critical point is measured by a parameter inversely proportional to the α power of the specific heat at constant magnetization, which is related to the fluctuations in energy density.¹ In our second representation, Eq. (6), the distance from the critical point is inversely proportional to the γ power of the susceptibility, and hence a measure of the fluctuations in magnetization. Behavior in the critical region is determined by the divergence of fluctuations as the critical point is

approached, and we presume this is why these two equations of state are reasonably satisfactory.

We do not understand why Eq. (5) is preferable to Eq. (6) for CrBr_3 . There is no reason to assume that either Eq. (5) or Eq. (6) represents the precise analytic form of the equation of state; however, these must be reasonably good approximations to the correct equation. Recent calculations for the three-dimensional Ising model³⁰ suggest that Eq. (5) is not precisely correct; however, it is indeed very good, agreeing to better than 1% with approximate calculations for this particular model.

The same equation provides an equally impressive fit to experimental data for real systems and is in a form quite suitable for engineering calculations of the thermodynamic properties of magnets, pure fluids, and possibly other systems in the critical region. Recently it has been successfully used³¹ to correct for the effects of gravity on measurements of specific heat and sound velocity in several fluids near the critical point. Only five parameters are required to represent the experimental data and these may be obtained from relatively few measurements. For example, a measurement of the spontaneous magnetization below T_c , and the susceptibility along the critical isochore above T_c , is sufficient to determine the entire equation of state.

ACKNOWLEDGMENTS

We are grateful to Dr. A. C. Linz for our samples of CrBr_3 and to Dr. Peter Schofield for a fruitful collaboration on the parametric approach to the equation of state. We have benefited from helpful discussions with Professor George B. Benedek and Professor Michael J. Stephen.

APPENDIX A: THEORY OF POLARIMETER

The light intensity I at a detector separated from the source by a pair of nearly crossed polarizers is given by

$$I = I_0 \sin^2 \theta + I_l, \quad (\text{A1})$$

where $(I_0 + I_l)$ is the intensity when the polarizers are parallel, I_l is the leakage intensity at the null position, and θ is the angular deviation in radians of the polarizer axes from the null. If the polarization of the light is further modulated at an angular frequency ω and an amplitude θ_0 , the intensity becomes

$$I = I_0 \sin^2(\theta + \theta_0 \sin \omega t) + I_l. \quad (\text{A2})$$

If $\theta_0 \ll 1$, Eq. (2) can be expanded in power series in θ_0 :

$$I = I_l + \frac{1}{2} I_0 \{ 1 - \cos 2\theta [(1 - \theta_0^2) + \theta_0^2 \cos 2\omega t + \dots] + \sin 2\theta [(2\theta_0 - \theta_0^3) \sin \omega t + \frac{1}{3} \theta_0^3 \sin 3\omega t + \dots] \}. \quad (\text{A3})$$

The amplitude I_ω of the intensity component at frequency ω is

$$I_\omega = \frac{1}{2} I_0 (2\theta_0 - \theta_0^3) \sin 2\theta. \quad (\text{A4})$$

This is the source of the signal at the lock-in detector and goes through zero at the null position.

The shot noise N in the photocurrent is proportional to the square root of the dc signal and is given by

$$N^2 = \alpha B (I_l + \frac{1}{2} I_0 \theta_0^2), \quad (\text{A5})$$

where α is the emission rate of photoelectrons per unit I and B is the bandwidth of the lock-in detector. The amplitude S of the signal component (at frequency ω) of the photocurrent is approximately

$$S = 2\alpha I_0 \theta \theta_0. \quad (\text{A6})$$

Thus the signal to noise ratio is

$$(S/N)^2 = 4\alpha I_0^2 \theta^2 \theta_0^2 / (I_l + \frac{1}{2} I_0 \theta_0^2) B. \quad (\text{A7})$$

If $\theta_0^2 \ll 2I_l/I_0$, we have

$$S/N = 2\theta (\alpha I_0/B)^{1/2} \theta_0 (I_0/2I_l)^{1/2}. \quad (\text{A8})$$

On the other hand, if $\theta_0^2 \gg 2I_l/I_0$, we have

$$S/N = 2\theta (\alpha I_0/B)^{1/2}. \quad (\text{A9})$$

Thus for sufficiently strong modulation, the signal-to-noise ratio is independent of the modulation amplitude and is related to the number of photoelectrons emitted in time $1/B$ with the polarizers uncrossed. The optimum modulation is

$$\theta_0^2 \simeq 4I_l/I_0.$$

APPENDIX B: FARADAY ROTATION IN CrBr_3

The origin of the large Faraday rotation in CrBr_3 was first discussed by Dillon, Kamimura, and Remeika.²² It was shown that at low temperatures the rotation is caused by the spin-orbit splitting of the excited states and is independent of the applied field as long as the sample is magnetically saturated.

A general theoretical treatment for the form of the electric dipole rotation due to magnetic ions in various circumstances has been given by Crossley *et al.*³² We will simply outline the approach and point out those features which are applicable to CrBr_3 .

The total Hamiltonian acting on the system is $H = H_0 + H_1$, where H_0 is the free-ion Hamiltonian together with the octahedral crystal field, and H_1 is the perturbation given by

$$H_1 = V_{CR} + V_{LS} - g\mu_B S_z H_{ex}. \quad (\text{B1})$$

Here V_{CR} is the small trigonal component of the crystal field, which is proportional to $1 - L_z^2$, V_{LS} is the spin-orbit interaction, and H_{ex} is the sum of the exchange field (using the molecular-field approximation for simplicity) and any external magnetic field. The ground states of the Cr^{3+} ion consist of the orbital singlet 4A_2 with a small admixing with the first excited states n , the orbital triplet 4T_2 , both having spin $S = \frac{3}{2}$.²² Let E_g^0 and E_n^0 be the unperturbed energies of the ground and excited states, respectively, and E_g and E_n the perturbation energies about the unperturbed values,

such that

$$|E_n|, |E_g| \ll E_n^0 - E_g^0 \equiv \hbar\omega_0. \quad (\text{B2})$$

The specific rotation θ in the absence of damping is given by

$$\theta = (\omega/2c)(n^- - n^+), \quad (\text{B3})$$

where ω is the angular frequency of the light, and n^+ and n^- are the refractive indices for right and left circularly polarized light, respectively. Applying the Kramers-Heisenberg dispersion relation and the Lorentz-Lorenz correction, this becomes

$$\theta = -K \sum_{\theta, n} [\omega^2 / (\omega_{n\theta}^2 - \omega^2)] \times [|\langle g | V_+ | n \rangle|^2 - |\langle g | V_- | n \rangle|^2] \rho_\theta, \quad (\text{B4})$$

where

$$K \equiv 2N(\bar{n} + 2)/9\bar{n}c\hbar, \quad (\text{B5})$$

$$\hbar\omega_{n\theta} \equiv \hbar\omega_0 + (E_n - E_\theta), \quad (\text{B6})$$

N is the number of ions per unit volume, \bar{n} is the mean refractive index, V_+ and V_- are the electric dipole operators for right and left circular polarization, respectively, and ρ_θ is the occupation probability of the ground state g .

In the conditions under consideration,

$$|\omega_0^2 - \omega^2| \gg \omega_0 |E_n - E_\theta| / \hbar.$$

Therefore the frequency-dependent factor in Eq. (B4) can be expanded in the form

$$\frac{\omega^2}{\omega_{n\theta}^2 - \omega^2} = \frac{\omega^2}{\omega_0^2 - \omega^2} \left[1 - \frac{2(E_n - E_\theta)\omega_0}{\hbar(\omega_0^2 - \omega^2)} + \dots \right] \quad (\text{B7})$$

and we obtain the first three terms in the formula for θ :

$$\theta_1 = -K [\omega^2 / (\omega_0^2 - \omega^2)] \times \sum_g \rho_g \sum_n [|\langle g | V_+ | n \rangle|^2 - |\langle g | V_- | n \rangle|^2], \quad (\text{B8})$$

$$\theta_2 = -K [2\omega^2\omega_0 / \hbar(\omega_0^2 - \omega^2)^2] \times \sum_g \rho_g E_g \sum_n [|\langle g | V_+ | n \rangle|^2 - |\langle g | V_- | n \rangle|^2], \quad (\text{B9})$$

$$\theta_3 = K [2\omega^2\omega_0 / \hbar(\omega_0^2 - \omega^2)^2] \times \sum_g \rho_g \sum_n [|\langle g | V_+ | n \rangle|^2 - |\langle g | V_- | n \rangle|^2] \langle n | H_1 | n \rangle. \quad (\text{B10})$$

It can be shown³² that if the ground state is regarded as a pure orbital singlet, θ_1 and θ_2 vanish. When the perturbation H_1 in Eq. (B1) is substituted to evaluate θ_3 , only the V_{LS} term contributes. Using the form

$$V_{LS} = \sum_i \lambda_i \mathbf{L} \cdot \mathbf{S}, \quad (\text{B11})$$

where the summation is over the three electrons in the ion and λ_i are the spin-orbit coupling constants, and defining a projection operator P such that for any

wave function Ψ

$$P|\Psi\rangle = \sum_{m=-l}^{m=l} \langle l, m | \Psi \rangle |l, m\rangle, \quad (\text{B12})$$

where $|l, m\rangle$ are angular momentum eigenfunctions, one obtains the expression

$$\theta_3 = K_3 \lambda [\omega^2\omega_0 / \hbar(\omega_0^2 - \omega^2)^2] M, \quad (\text{B13})$$

with

$$M \equiv N\mu_B \sum_{m=-3/2}^{m=3/2} \rho_m m, \quad (\text{B14})$$

$$\lambda \equiv \frac{1}{3} \sum_i \lambda_i, \quad (\text{B15})$$

and

$$K_3 \equiv (4K/N\mu_B) \sum_i (\lambda_i/\lambda) \langle {}^4A_2 | V_+ P L_{iz} P V_- | {}^4A_2 \rangle. \quad (\text{B16})$$

M defined in Eq. (B14) is the magnetization of the sample, and depends on H_{ex} through ρ_m .

In reality, the ground states have the form

$$|g\rangle = |{}^4A_2\rangle - \alpha(\Delta g/g) m |{}^4T_2\rangle, \quad (\text{B17})$$

where α is a number of the order of unity and Δg is the deviation of the Lande g factor from the spin-only value. Then θ_1 and θ_2 have finite contributions, the former being predominant because of the frequency-dependent factor and given by

$$\theta_1 = K_1 (\Delta g/g) [\omega^2 / (\omega_0^2 - \omega^2)] M, \quad (\text{B18})$$

where

$$K_1 \equiv (2\alpha K/N\mu_B) \langle {}^4A_2 | (V_+ P V_-) - (V_- P V_+) | {}^4T_2 \rangle. \quad (\text{B19})$$

Since Δg is about 0.01 for CrBr_3 ,³³ we expect θ_1 to be substantial and may even be of the same order as θ_3 .

Thus for CrBr_3 the Faraday rotation can be separated into the two terms in Eq. (B13) and Eq. (B18), both linear in the magnetization, with coefficients which have different frequency dependence but are both temperature independent. Higher-order terms in the expansion in Eq. (B7) give nonlinear contributions, but these are reduced by at least the factor E_n/ω_0 , which is of the order of 10^{-3} .

APPENDIX C: EQUATIONS IN LINEAR MODEL

Here we summarize expressions for various thermodynamic quantities using the parametric equation of state Eq. (5). This is called the "linear model" in Ref. 26. We begin with a general statement of thermodynamics in the critical region using parametric notation. It is convenient to define a potential $\pi(r, \theta)$ which

depends upon the parameters r and θ . From this one may calculate

$$M(r, \theta) = \left(\frac{\partial \pi}{\partial H} \right)_T = \frac{\partial(\pi, T)}{\partial(r, \theta)} \bigg/ \frac{\partial(H, T)}{\partial(r, \theta)}, \quad (\text{C1})$$

$$S(r, \theta) = \left(\frac{\partial \pi}{\partial T} \right)_H = \frac{\partial(\pi, H)}{\partial(r, \theta)} \bigg/ \frac{\partial(T, H)}{\partial(r, \theta)}, \quad (\text{C2})$$

where S is the critical part of the entropy. Other quantities may be calculated in a similar manner. If we now include the experimentally observed power laws in the form of the r dependence of the functions, we obtain

$$\pi(r, \theta) = p(\theta) r^{\beta\delta + \beta}, \quad (\text{C3a})$$

$$M(r, \theta) = m(\theta) r^\beta, \quad (\text{C3b})$$

$$H(r, \theta) = h(\theta) r^{\beta\delta}, \quad (\text{C3c})$$

$$T(r, \theta) = t(\theta) r, \quad (\text{C3d})$$

$$S(r, \theta) = s(\theta) r^{\beta\delta + \beta - 1}. \quad (\text{C3e})$$

Substituting these into Eqs. (C1) and (C2), one obtains

$$\pi = [\delta/(\delta+1)]MH + [1/\beta(\delta+1)]TS \quad (\text{C4a})$$

or, in alternate form,

$$p(\theta) = [\delta/(\delta+1)]m(\theta)h(\theta) + [1/\beta(\delta+1)]t(\theta)s(\theta). \quad (\text{C4b})$$

Equation (C1) can be written as

$$\{t^{-\beta\delta - \beta}g\}' = \beta\delta m h t^{-\beta\delta - \beta - 1}t' - m h' t^{-\beta\delta - \beta}. \quad (\text{C5})$$

In Eq. (C5) the prime denotes differentiation with respect to θ and the θ dependence of the functions m , h , and t is not shown explicitly.

If the specific forms for m , h , and t given in Eq. (5) are chosen, then Eq. (C5) may be readily integrated to obtain an expression for $p(\theta)$. One may then obtain an expression for $s(\theta)$ by substituting in Eq. (C4b) and calculate the specific heat from Eq. (C2) in the form

$$C_M = (\beta\delta + b - 1)(S/T) - \beta(M/T)(\partial S/\partial M)_T. \quad (\text{C6})$$

If one requires that C_M be independent of θ , one obtains an equation whose solution is given by Eq. (5d).

On the other hand, if it is desired to make the susceptibility independent of θ , one readily obtains Eq. (6). The results summarized in Eqs. (C4)–(C6) are generally true for the power-law dependences in Eq. (C3) and may be used to calculate other thermodynamic derivatives even if different forms for $m(\theta)$, $t(\theta)$, and $h(\theta)$ are chosen.

† Work supported by the Advanced Research Projects Agency, under Contract No. SD-90, and by the National Aeronautics and Space Administration under Grant No. NGR-22-009-182.

¹ Leo P. Kadanoff *et al.*, *Rev. Mod. Phys.* **39**, 395 (1967).

² P. Heller, *Rept. Progr. Phys.* **30**, 731 (1967).

³ M. E. Fisher, *Rept. Progr. Phys.* **30**, 615 (1967).

⁴ L. D. Landau, English translation and Russian references may be found in *Collected Papers of L. D. Landau*, edited by D. ter Haar (Gordon and Breach, New York, 1965), p. 193.

⁵ B. Widom, *J. Chem. Phys.* **43**, 3898 (1965).

⁶ Leo P. Kadanoff, *Physics* **2**, 263 (1966).

⁷ R. B. Griffiths, *Phys. Rev.* **158**, 176 (1967).

⁸ A. Arrott and J. E. Noakes, *Phys. Rev. Letters* **19**, 786 (1967).

⁹ J. S. Kouvel and J. B. Comly, *Phys. Rev. Letters* **20**, 1237 (1968).

¹⁰ J. S. Kouvel and D. S. Rodbell, *Phys. Rev. Letters* **18**, 215 (1967).

¹¹ M. S. Green, M. Vicentini-Missoni, and J. M. H. Levelt Sengers, *Phys. Rev. Letters* **18**, 1113 (1967).

¹² J. T. Ho and J. D. Litster, *J. Appl. Phys.* **40**, 1270 (1969).

¹³ J. T. Ho and J. D. Litster, *Phys. Rev. Letters* **22**, 603 (1969).

¹⁴ P. Schofield, *Phys. Rev. Letters* **22**, 606 (1969).

¹⁵ B. D. Josephson, *J. Phys. C* **2**, 1113 (1969).

¹⁶ I. Tsubokowa, *J. Phys. Soc. Japan* **15**, 1664 (1960).

¹⁷ A. C. Gossard, V. Jaccarino, and J. P. Remeika, *Phys. Rev. Letters* **7**, 122 (1962).

¹⁸ H. L. Davis and A. Narath, *Phys. Rev.* **134**, A433 (1964).

¹⁹ S. D. Senturia and G. B. Benedek, *Phys. Rev. Letters* **17**, 475 (1966).

²⁰ L. G. Gouy, *Compt. Rend.* **109**, 935 (1889).

²¹ S. Foner, *Rev. Sci. Instr.* **30**, 548 (1959).

²² J. F. Dillon, Jr., H. Kamimura, and J. P. Remeika, *J. Appl. Phys.* **34**, 1240 (1963).

²³ J. S. Kouvel and M. E. Fisher, *Phys. Rev.* **136**, A1626 (1964).

²⁴ F. J. Cadieu, and D. H. Douglass, Jr., *Phys. Rev. Letters* **21**, 580 (1968).

²⁵ M. Vicentini-Missoni, J. M. H. Levelt Sengers, and M. S. Green, *Phys. Rev. Letters* **22**, 389 (1969).

²⁶ P. Schofield, J. D. Litster, and John T. Ho, *Phys. Rev. Letters* **23**, 1098 (1969).

²⁷ J. T. Ho and J. D. Litster (unpublished).

²⁸ B. Chu, F. J. Schoenes, and M. E. Fisher, *Phys. Rev.* **185**, 219 (1969).

²⁹ G. B. Benedek, in *Polarisation Matière et Rayonnement, Livre de Jubilé et l'honneur du Professeur A. Kastler* (Presses Universitaires de Paris, France, 1968).

³⁰ D. S. Gaunt and C. Domb, *J. Phys. C* (to be published).

³¹ M. Barmatz and P. C. Hohenberg, *Phys. Rev. Letters* **24**, 1225 (1970).

³² W. A. Crossley, R. W. Cooper, J. L. Page, and R. P. van Staple, *Phys. Rev.* **181**, 896 (1969).

³³ J. F. Dillon, Jr., *J. Appl. Phys.* **33**, 1191 (1962).